Ratiometric Analysis of Fluorescence Lifetime for Probing Binding Sites in Albumin with Near-Infrared Fluorescent Molecular Probes

Mikhail Y. Berezin[1], Hyeran Lee[1], Walter Akers[1], Gregory Nikiforovich[2] and Samuel Achilefu*[1]

[1]Department of Radiology, Washington University School of Medicine, St. Louis, MO
[2]Department of Biochemistry and Molecular Biophysics, Washington University School of Medicine, St. Louis, MO

ABSTRACT

A number of diseases have been linked to abnormal conformation of albumin, a major extracellular protein in blood. Current protein structural analysis requires pure isolated samples, thereby limiting their use for albumin analysis in blood. In this study, we report a new approach for high-throughput structure-related analysis of albumin by using the fluorescence lifetime properties of near-infrared (NIR) polymethine dyes. Based on molecular modeling, polymethine dyes are bound to two binding sites with different polarities on albumin. As a result, an NIR molecular probe exhibits two distinct lifetimes with two corresponding fluorescent fractional contributions. The distribution of fractional contributions along with individual fluorescence lifetimes represents unique parameters for characterizing albumin architecture by ratiometric analysis. After screening a small library of NIR polymethine dyes, we identified and used a polymethine dye with optimal fluorescence lifetime properties to assess structure-related differences in commercially available bovine serum albumin as model systems. The results show that changes in the lifetime of NIR dyes reflect the perturbation of the tertiary structures of albumin and that albumin prepared by different methods has slightly altered tertiary structures. Because of the reduced absorption of light by blood in the NIR region, the method developed can be used to determine structural changes in albumin in whole blood without prior isolation of the pure protein.

INTRODUCTION

Serum albumin, the major extracellular multifunctional protein in mammals, is a multifunctional protein involved in many critical physiological processes. These include the binding and transport of exogenous and endogenous ligands, maintenance of colloidal osmotic pressure, free-radical scavenging (1), regulations of acid–base balance, coagulation processes and vascular permeability. Despite its rigid structure secured by 17 disulfide bonds, albumin can undergo structural modifications *via* oxidative and nonoxidative pathways (2), leading to anomalous conformations and changes in binding properties. The alternations in albumin structure have been linked to patients with cirrhosis (3), diabetes, renal disease (4), aging, acute and chronic inflammation, acute schizophrenia (5) and cancer (6). Therefore, knowledge of the structural status of albumin could provide early manifestation of disease and prevent serious complications. To obtain such information, a high-throughput method for analyzing albumin, preferably without its separation from whole blood, is highly desirable.

Given the importance of albumin in many vital processes, the characterizations of its overall structure and binding sites' have been the focus of many studies (7). In addition to the traditional direct analytical structural techniques (X-ray crystallography, nuclear magnetic resonance [NMR], circular dichroism [CD]), indirect methods based on the use of specific markers and molecular probes for binding sites' characterization have emerged. For example, the structure of albumin has been analyzed with spin-probes by electron spin resonance spectroscopy (6), unsaturated fatty acids' probes by mass spectrometry (8), solvatochromic fluorescent dyes by steady-state emission spectroscopy and intrinsic albumin fluorophores (tryptophans) by time-resolved fluorometry. The last method capitalizes on the sensitivity of tryptophan's fluorescence lifetime to the surrounding medium (9) and the low abundance of tryptophan in albumin. However, this method is not suitable for high-throughput screening of albumin because of the need for pure sample that is not contaminated with other fluorophores. Moreover, high-scattering UV light used to excite tryptophans (10) as well as the quenching of tryptophan fluorescence can compromise the data in whole blood. For these reasons, using endogenous environment-sensitive fluorophores for probing albumin is less attractive in heterogeneous biological systems.

Near-infrared (NIR) polymethine dyes, such as indocyanine green (ICG) and its structural analogs, are widely used in optical imaging *in vivo* because of the low absorption of light by blood and endogenous chromophores, resulting in low autofluorescence and high detection sensitivity (11). With the recent advances in synthetic polymethine dye chemistry (12), diverse NIR dyes can be tailored for specific applications. These NIR polymethine dyes are particularly attractive for probing heterogeneous media because of their high extinction coefficients and fluorescent quantum yields (when confined in a rigid biological matrix such as albumin binding sites), monoexponential decays in homogeneous media and sensitivity of their fluorescence lifetimes to the immediate environment. Moreover, lifetime is insensitive to the dye concentration, which minimizes the effects of concentration artifacts and photobleaching (13) and is less affected by the excitation intensity. It is largely unaffected by light scattering (14) and

sample turbidity (15), which are critical drawbacks for steady-state fluorometry with whole blood. Thus, a combination of the NIR optical properties of polymethine dyes with the sensitivity of fluorescence lifetime measurements to their local environment represents a powerful and sensitive method to study biological analytes.

In this report, we describe a new approach for high-throughput structural analysis of albumin with NIR polymethine dyes by using ratiometric analysis of fluorescence lifetime (RAFL). The principle of the new approach is based on the observation that a polymethine NIR probe bound to albumin exhibits two-exponential decay (Eq. 1) with two distinct lifetimes and two corresponding fluorescent fractional contributions (Eq. 2).

$$I(t) = \sum_{i}^{n} \alpha_i \exp(-t/\tau_i) \qquad (1)$$

$I(t)$ is intensity as a function of time, τ_i is the decay time of the component i, α_i is the amplitude of the component i at $t = 0$ and n is the number of components equal to 2.

$$\begin{aligned} f_a &= \alpha_a \tau_a / (\alpha_a \tau_a + \alpha_b \tau_b) \times 100 \\ f_b &= \alpha_b \tau_b / (\alpha_a \tau_a + \alpha_b \tau_b) \times 100 \end{aligned} \qquad (2)$$

f_a and f_b are the fractional components (%) with lifetimes τ_a and τ_b (ns) with amplitudes α_a and α_b.

Computational analysis of NIR polymethine dye, cypate, complexed to albumin revealed two binding sites with different polarities. Therefore, the two distinct lifetimes and the corresponding fluorescent fractional contributions would reflect changes in albumin tertiary structure. By screening a small library of NIR polymethine dyes available commercially or prepared in our laboratory, we have identified molecular probes that could be employed in RAFL. One of the probes was used to illustrate the differences between commercially available bovine serum albumin (BSA) prepared by different methods.

MATERIALS AND METHODS

Materials. Near-infrared dyes ICG, IR-820, IR-806, IR-786 and DTTCI were purchased form Sigma-Aldrich (St. Louis, MO). Cypate, LS-276, LS-277, LS-287, LS-288 and LS-319 were synthesized as described previously (12,16,17). BSA (cat. no. A3059, A3294, A6003, A 9647, and A-4378; Sigma-Aldrich), dimethyl sulfoxide (DMSO) and urea (Fisher Scientific, Hampton, NH) and 2-mercaptoethanol (Bio-Rad Laboratories, Hercules, CA) were purchased from commercial sources. Millipore 18.2 water MΩ·cm was used throughout the work. All commercial chemicals were used without further purification and solvents (ACS grades) were not degassed.

Sample preparations. Bovine serum albumin (50 mg) was dissolved in 1 mL of 0.01 M phosphate-buffered saline (PBS; Sigma-Aldrich). This concentration of albumin in solution reflects the normal physio-logical concentration of albumin in human plasma (18). Dyes were dissolved in 150 μL to obtain 50–100 μM concentration in DMSO and kept as stock solutions at −20°C wrapped in foil. Aliquots were added to albumin-PBS solution (1 mL) and the mixtures were vortexed for 1 min. To prevent inner filter effect, the samples were then diluted with PBS buffer to adjust the UV–Vis absorbance to 0.1–0.3. For albumin unfolding–refolding study, 50 mg of BSA was dissolved in 1 mL of 6 M urea in water and 5 μL of cypate in DMSO was added. The solution was adjusted to 0.1 absorbance with 6 M urea or water (the adjusted water solution was 0.4 M urea). 2-Mercaptoethanol (10 μL) was added to the BSA-cypate in 6 M urea solution . All mixtures were vortexed for at least 1 min to ensure complete mixing.

Steady-state spectra. The absorption spectra were recorded on a Beckman Coulter DU 640 spectrophotometer (Fullerton, CA) and fluorescence steady-state spectra on a Fluorolog III fluorometer (Horiba Jobin Yvon, Edison, NJ) with 720 nm excitation and 5 nm slits. All measurements were conducted at room temperature.

Fluorescence lifetime measurement. The fluorescence lifetime was measured using the time-correlated single-photon-counting (TCSPC) technique (Horiba) with excitation source NanoLed® 773 nm impulse repetition rate 1 MHz (Horiba) at 90° to the R928P detector (Hamamatsu Photonics, Japan). The detector was set to 820 nm with a 20 nm bandpass. The electrical signal was amplified by TB-02 pulse amplifier (Horiba) and the amplified signal was fed to the constant fraction discriminator CFD (Philips, The Netherlands). The first detected photon was used as a Start signal by time-to-amplitude converter (TAC), the excitation pulse triggered the Stop signal. The multichannel analyzer (MCA) recorded repetitive start–stop signals from the TAC and generated a histogram of photons as a function of time-calibrated channels (6.88 ps/channel) until the peak signal reached 10 000 counts. The lifetime was recorded on a 50 ns scale. The instrument response function was obtained using Rayleigh scatter of Ludox-40 (0.03% in MQ water; Sigma-Aldrich) in a quartz cuvette at 773 nm emission. The measurements were conducted at room temperature. DAS6 v6.1 decay analysis software (Horiba) was used for lifetime calculations. The goodness of fit was judged by chi-squared values, Durbin–Watson parameters and visual observations of fitted line, residuals and autocorrelation function. Three-exponential decay equations were used for data fitting. In all cases lifetime components with insignificant contribution (<3%) were discarded and decays were considered to be two-exponential. The remaining lifetime components were used for further analysis. All samples were analyzed in triplicates using new solutions to avoid reanalyzing the same sample.

Molecular modeling. The albumin–dye interactions were modeled in two steps. First, cypate molecule was docked to the X-ray structure of albumin (the PDB entry 1AO6) employing the GRAMM program for low-resolution docking (19). GRAMM performed systematic sampling of all possible binding modes of cypate to albumin on the six-dimensional grid of the three orthogonal translational axes with the grid step of 3 Å and of three rotations around these axes with the grid step of 20°. Sampling was performed in several runs with different sets of adjustable parameters of the GRAMM procedure. Spatial distribution of the cypate binding modes that correspond to highest values of the scoring function used by GRAMM converged to two main binding sites with increasing of the value of a specific "repulsion" parameter. Second, typical binding modes for cypate in each of the found sites were selected, and the corresponding complexes of albumin and cypate molecules were subjected to energy minimization in the SYBYL software package (Tripos Inc., St. Louis, MO), which eliminated possible steric clashes between cypate and albumin.

RESULTS AND DISCUSSION

Optimizing measurement conditions with cypate

Cypate (16,20) is a reactive structural analog of ICG that is widely used in optical imaging because of its valuable NIR optical properties. In this study, cypate was used as a standard to optimize albumin-binding conditions for lifetime measure-ment and evaluate reproducibility of the data. In the first set of experiments, the lifetime of albumin–cypate complex (molar ratio albumin–cypate 11:1, albumin: cat. no. A3059, Sigma-Aldrich) in PBS at different concentrations from 0.5 to 10 mg mL^{-1} was measured. The range of concentrations was chosen to provide adequate signal at low concentrations while maintaining a photon count rate between 0.3% and 2%, and to avoid pile-up effect (21) at high concentrations. The results shown in Table 1 demonstrate that cypate exhibits two major lifetime components of 0.47 and 0.95 ns denoted here as τ_a and τ_b, respectively, with fractional contribution $f_a = 69\%$ and $f_b = 28\%$. Both the lifetimes and fractional contributions are

Table 1. Effect of concentration of albumin–cypate complex in PBS on cypate fluorescence lifetime.

BSA–cypate complex, mg mL^{-1}	BSA-to-cypate ratio, mol mol^{-1}	τ_a, ns	f_a, %	τ_b, ns	f_b,%
0.5	11	0.46	66.34	0.92	31.02
2.5	11	0.48	70.79	0.97	26.62
5	11	0.48	72.04	0.96	25.19
10	11	0.46	68.71	0.94	28.27
Average*		0.47 ± 0.01	69.47 ± 2.50	0.95 ± 0.02	27.78 ± 2.50

*Average error expressed as standard deviation. PBS = phosphate-buffered saline; BSA = bovine serum albumin.

within statistically satisfactory range of 2.5% and indicate that lifetime measurements were independent of the concentration of albumin–cypate complex in solution.

In the second set of measurements, the concentration of albumin in cuvette was kept constant, and the amount of added cypate was varied. At low concentrations of cypate (cypate-to-albumin molar ratio from 1:1000 to 1:10), the lifetime of both components remained constant at 0.47 and 1.0 ns (Fig. 1a). At higher concentrations (cypate–albumin ratio > 1:10), the short lifetime component decreased from τ_a = 0.47 ns to τ_a = 0.2 ns, indicating the presence of unbound cypate in solution (fluorescence lifetime of cypate in water < 0.2 ns). In contrast, the lifetime of the long lifetime component was practically unaffected under similar conditions

(from τ_b = 1.1 ns at 1:1000 mol mol^{-1} to τ_b = 0.9 ns at 1:1 mol mol^{-1}). The fractional contributions are nearly independent of cypate-to-albumin ratio within the broad range between 1:1000 and 1:10 (Fig. 1b). At higher molar concentration of cypate, especially at 1:1 cypate–albumin stoichiometric ratio, changes in the fractional components were observed because of contribution from unbound cypate.

These results show that the two major lifetimes of cypate bound to albumin and their respective fractional contributions are independent of albumin–cypate concentration and in general to cypate–albumin ratios. Both lifetimes and their distributions therefore could be utilized for structural characterization of albumin. Based on the above findings, the lifetimes of a molecular probe upon binding to albumin could serve as a characteristic feature of the binding sites while the distribution, expressed as fractional contributions, would indirectly indicate the binding affinities of each albumin binding site to the probe. Together, these independent parameters (lifetimes and fractional contributions) could be used to characterize structural changes in albumin. To demonstrate the validity of this approach, the tertiary structure of albumin was perturbed to cause unfolding and refolding of the protein for studying changes in the above structural reporters.

Effect of unfolding–refolding on the lifetime of cypate in albumin

Having established that both lifetimes and their fractional contributions are concentration independent, we analyzed the changes in lifetime measurement of cypate in albumin under unfolding–refolding conditions. First, the albumin was partially unfolded with urea (6 M) (22) and then allowed to equilibrate with cypate. The results shown in Table 2 reflect significant changes in albumin structure from its native state. The lifetime of the short lifetime component changed from

(a)
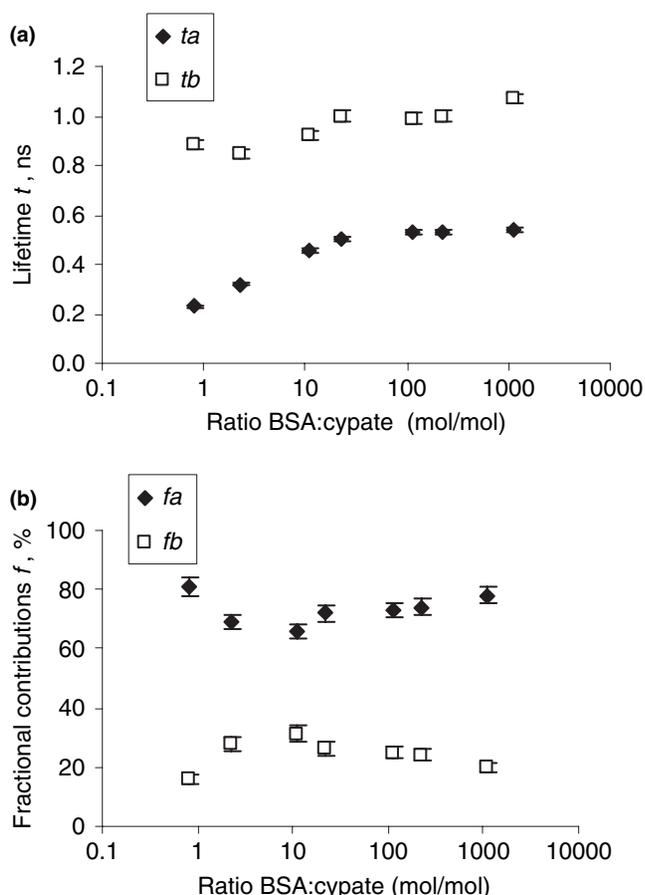
Figure 1. Fluorescence lifetimes (a) of cypate and (b) corresponding fractional contributions as a function of cypate-to-albumin ratio.

Table 2. Cypate lifetime in folded and unfolded state.

| Cypate in media	τ_a, ns	f_a, %	τ_b, ns	f_b, %
Cypate in albumin in urea 6 M in water	0.23	86	0.95	11
Cypate in albumin in 0.4 M urea in PBS buffer	0.53	80	1.1	17
Cypate in albumin in PBS buffer (no urea)	0.47	67	0.97	30
Cypate + albumin + 6 M urea + 2-mercaptoethanol in PBS	<0.2	93	–	–

PBS = phosphate-buffered saline.

0.47 to 0.23 ns, indicating almost complete disappearance of the short lifetime binding site and a significant decrease in the long lifetime contribution from $f_b = 36\%$ to $f_{b(\text{unfold})} = 11\%$. Subsequent treatment of partially unfolded albumin with 2-mercaptoethanol (23) disrupted the long lifetime binding pocket, thereby increasing the concentration of unbound cypate in solution, as shown by the presence of only one major (93%) lifetime component (< 0.2 ns). In addition, the dilution of 6 M urea in cypate–albumin solution with water to 0.4 M re-established the two lifetimes ($f_a = 0.53$ [80%] and $f_b = 1.1$ ns [17%]), indicating a restoration of both binding sites of albumin (not necessarily the same sites) *via* refolding. These results demonstrate that the lifetime of cypate and the distribution of the two sites could be used to monitor the changes in protein tertiary structure.

Screening a small library of NIR fluorescent dyes

A potential application of the lifetime method developed herein is to determine changes in the tertiary structures of albumin and other proteins in heterogeneous media such as blood. Consequently, we were interested in polymethine molecular probes that absorb and fluorescence in the NIR wavelengths between 700 and 900 nm to minimize autofluorescence and improve the detection sensitivity of the protein in blood. Ideally, the molecular probes should demonstrate mono-exponential decay in homogeneous solutions, respond to changes in its local environment with high sensitivity, possess high absorption coefficients and fluorescence quantum yields, and exhibit at least two distinct lifetime signals when bound to albumin, preferably with similar affinity toward binding sites. In addition, it is desirable that the fluorescence lifetimes are measurable with conventional frequency or time-domain spectrofluorometers. Routine determination of fluorescence lifetime of dyes has been made possible by the availability of inexpensive LED sources, in contrast to expensive pulsed lasers. However, relatively long pulse widths (773 nm Nanoled® pulse duration was 1.7 ns) compare with pico- and femto-second lasers making the measurement of lifetime shorter than 0.2 ns inaccurate and impractical with our system. With lifetimes longer than 0.2 ns, the signal to noise ratio, and therefore the accuracy of the lifetime measurements would significantly improve.

In this work, we screened 11 NIR polymethine dyes prepared in our laboratory and purchased from commercial sources. The primary goal of the screening was to identify an NIR dye that satisfies the above-mentioned requirements. All of the compounds examined absorb and emit light between 750 and 850 nm and have high molar absorptivity (200 000–220 000 $M^{-1} cm^{-1}$) and modest fluorescent quantum yield (0.05–0.10) in methanol. The quantum yield of the dyes significantly increases in the presence of albumin (up to 0.50) as it is shown in Fig. 2 for free cypate and cypate–albumin complex.

When cypate is bound to albumin in its native conformation, two major lifetime components are normally seen, a short lifetime ($f_a = 70$–77%) and a long lifetime ($f_b = 20$–27%). This distribution is not optimal for ratiometric analysis. In the ideal case, the distribution should be close to 50–50% so that small conformational changes could result in large changes in the ratio of the components. Furthermore,
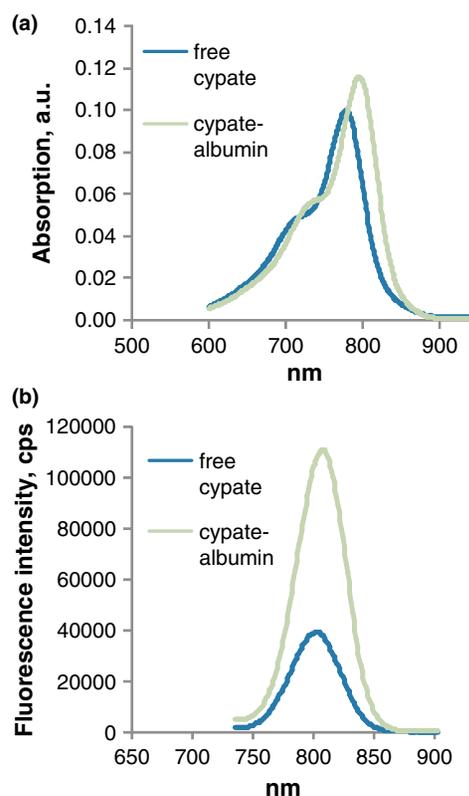
Figure 2. Steady-state absorbance (a) and emission spectra (b) of free cypate and cypate bound to albumin at the same cypate concentration (PBS buffer, ex. 720 nm).
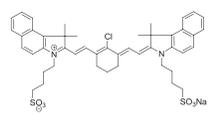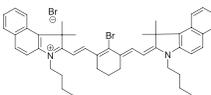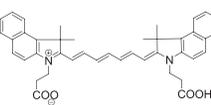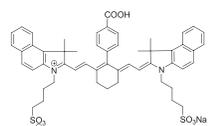
it is also desirable to have dyes with lifetimes longer than cypate to improve accuracy, and larger differences between lifetimes (for cypate $\tau_b - \tau_a \sim 0.5$ ns) to improve resolution. The former parameter is especially important from both the instrumentation point of view and applicability of the method to whole-blood screening.
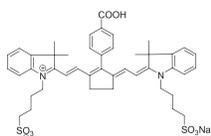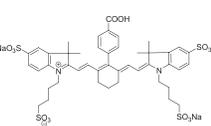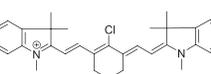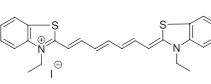
Similar to cypate, the majority of polymethine molecules studied after incubation with albumin exhibited a short (0.4–0.7 ns) and a long (0.9–1.3 ns) lifetime component (Table 3). The results indicate that, in general, NIR polymethine compounds tend to populate two binding sites. Based on the criteria of longer lifetime and equal distribution between the sites, LS-288 and LS-276 were found to be the best compounds, with LS-288 having the largest difference between short and long lifetimes (0.66 ns for LS-288 *vs* 0.50 ns for LS-276). Thus, LS-288 was chosen for probing the similarities of the tertiary structures of commercially available BSA prepared by different methods.

Evaluating the tertiary structures of bovine serum albumin

Bovine serum albumin produced by a number of methods collectively known as Cohn processes is widely used in diagnostics, cell culture, microbial culture and biochemical research. The Cohn process (24) was initially developed for obtaining pure albumin in large quantities as human plasma substitute during World War II and has undergone numerous modifications (25,26). The modern processes vary significantly.

Table 3. Fluorescence lifetime and fractional distributions of near-infrared dyes bound to bovine serum albumin.

Entry	Structure	τ_a, ns	f_a, %	τ_b, ns	f_b, %	$\tau_b - \tau_a$, ns	f_a/f_b
IR-820		0.41	77	0.91	19	0.50	4.1
LS-319		0.59	72	1.13	25	0.54	2.9
Cypate		0.47	69	0.97	30	0.50	2.2
LS-277		0.64	65	1.15	32	0.51	2.0
ICG		0.63	61	1.1	37	0.47	1.6
IR-806		0.52	60	1.19	38	0.67	1.6
LS-287		0.67	58	1.14	39	0.47	1.5
LS-276		0.69	55	1.19	42	0.50	1.3
LS-288		0.61	37	1.29	60	0.66	0.6
IR-786		0.46	28	1.22	71	0.76	0.4
DTTCI		1.14	95	–	–	–	0.0
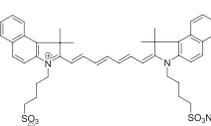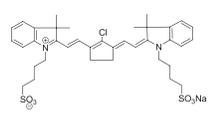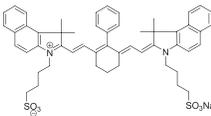
For example, cold alcohol precipitation method utilizes treatment of plasma with cold ethanol at −5 to −10°C, and in a heat shock method, the plasma is heated in ethanol to 68°C in the presence of stabilizers. To further increase the purity of the product, albumin is often extra-purified using organic solvent precipitations, crystallizations, chromatography and other methods. While the objective of the commercial processes is to keep the structural integrity of a protein intact, certain treatments might potentially cause an alteration in proteins' tertiary structure.

**Table 4.** Evaluation of bovine serum albumin prepared by different methods (http://www.sigmaaldrich.com).

Sigma-Aldrich catalog number	Initial isolation method	Further purification method	Purity (by agarose gel electrophoresis)
A3294	Heat shock	Further purified fraction V	≥98%, protease essentially free
A3059	Heat shock from pasteurized serum	Organic solvent precipitation	∼99%, essentially γ-globulin free
A6003	Cold alcohol precipitation		≥96%, essentially fatty acid free
A9647	Heat treatment	Organic solvent precipitation	≥96%, pH ∼7 (1 % [wt/vol] in H_2O)
A4378	Cold alcohol precipitation; prepared using method IV of Cohn	1 × crystallized using decanoic acid and ethanol	≥97%
A4503	Cold alcohol precipitation; prepared by a modification of Cohn, using cold ethanol and pH		≥96%

We analyzed six albumin samples available from Sigma-Aldrich (http://www.sigmaaldrich.com) prepared by different methods (Table 4). The results shown in Fig. 3 reflect small but statistically significant deviations in protein structures across the samples. In general, lifetime changes in the short lifetime pockets were more prominent relative to the long lifetime pockets, indicating that the former regions are more sensitive to albumin preparation. For example, albumin A6003 obtained by initial fractionation from cold alcohol has a lifetime of 0.70 ± 0.02 ns in its short lifetime region, whereas albumin A3294 prepared by initial treatment with a heat shock method has 0.57 ± 0.02 ns lifetime. At the same

time, the molecular probe in albumin A9647 prepared by the heat shock method showed the same lifetimes and lifetime distribution as in A4503 prepared by cold alcohol precipitation method. These results suggest that despite the differences in the production methods, the tertiary structures of some albumin are similar. Among the tested albumin, A6003 shows the largest deviation from the average lifetime distribution $f_a = 43.4 \pm 2.6\%$ and $f_b = 53.3 \pm 2.5\%$ with the average $f_a = 39.9 \pm 2.4\%$ and $f_b = 57.3 \pm 3.4\%$ for all other samples. Unfortunately, we were not able to test different batches of the A6003 to make a conclusive determination that the manufacturing process affected the structure. Regardless of speculations regarding the source of deviations, the results clearly show that NIR fluorescence lifetime method could be used to test the quality and reproducibility of albumin. Thus, we can use the method to detect major changes such as those found during the unfolding–refolding processes as well as small changes in tertiary structures of proteins.

Molecular modeling studies

Previously studies have shown that many fluorescent compounds with mono-exponential decays in homogeneous solution exhibit multiexponential decays when bound to albumin, indicating the presence of several binding regions (27–33). Since the early work of Sudlow *et al.* (34) who described two major binding sites known as Sudlow's sites I and II, several additional sites have been found (35–38). It was also suggested that albumin has certain conformational plasticity upon drug binding (39). Most of the fluorescent probes described in the literature and in the current work exhibit two lifetimes when bound to albumin. However, two lifetimes does not necessarily imply that the dye occupied only two binding sites. A typical deconvolution software based on least square fitting algorithm cannot accurately resolve the total fluorescence decay into individual components if three or more lifetimes are present. Instead, the obtained individual lifetimes would represent an average of several lifetimes leading to erroneous conclusion that the fluorescent compound is bound to fewer sites. Thus, it is important to answer a fundamental question: how many sites are actually occupied by the NIR fluorescent molecules? The answer would provide evidence for the number of expected lifetimes. In general, longer lifetime typically corresponds to more hydrophobic binding region, while shorter lifetime points to a hydrophilic region (27).
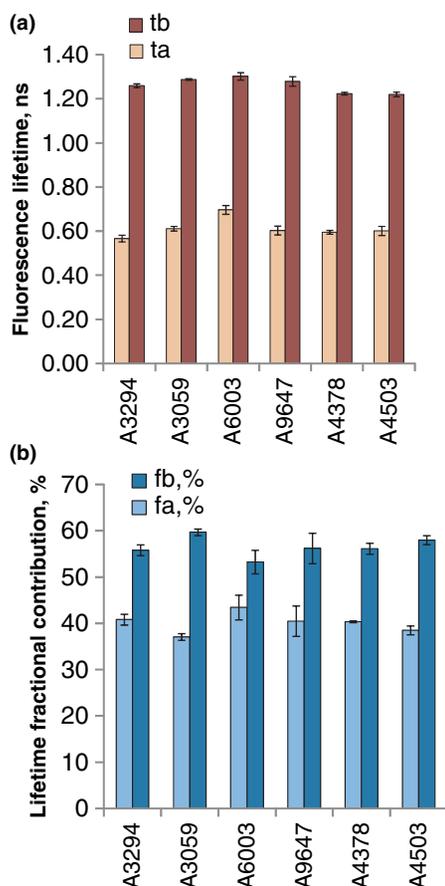
Figure 3. Fluorescence lifetime (a) and fluorescence fractional contributions (b) of LS-288 bound to bovine serum albumin prepared by different methods (*x*-axis: catalog numbers from Sigma-Aldrich).
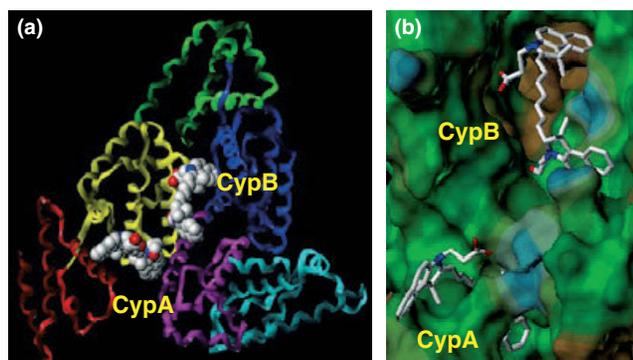
Figure 4. (a) Positions of two molecules of cypate in complex with albumin (binding sites CypA and CypB). Albumin domains are shown as shadow ribbons as follows: domain A in cyan, B in magenta, C in blue, D in green, E in yellow and F in red. Cypate molecule is shown as space-filled atoms. Hydrogen atoms are omitted. (b) Zoom of the two binding sites. Albumin surface is colored according to values of hydrophilic potential from brown (hydrophobic) to blue (hydrophilic).

In our computational study, cypate was chosen as a model because it has previously been used for molecular modeling study (40) and its geometry (size, planarity) is very similar to all other polymethine dyes used throughout this work. Two binding sites were found by molecular modeling, using cypate docking into the X-ray structure of albumin (the PDB entry 1AO6). Of the two binding sites found for cypate, the first site (CypA) is adjacent to the second one (CypB) and is formed by albumin helices B4, E3 and F2, as well as by short nonhelical segment connecting domains A and B (Fig. 4a). The second site (CypB) was a major one (about 80% of cypate configurations with high scores). It is located in the groove between domains B, C and E of albumin (see Fig. 4a) and is formed mainly by the following helices of albumin: B3, B4, C2, C6, E3 and E4. Site CypB is larger in size and more hydrophobic than site CypA (see Fig. 4b, where different colors represent different values of hydrophilic potential at the albumin surface in the vicinity of the sites). As site CypA is more hydrophilic than site CypB, we suggest that cypate bound to CypA exhibits a shorter lifetime (denoted above as τ_a), whereas cypate bound to CypB possesses a longer lifetime (τ_a).

Comparison with all available X-ray structures of albumin co-crystallized with various drugs and fatty acids (10 PDB entries with resolution equal or better than 2.4 Å) revealed that in most cases binding sites characteristic for fatty acids and small-size drugs do not coincide with sites CypA and CypB, as suggested in this study for cypate (data not shown). This is quite understandable because cypate has much larger size than most of the co-crystallized compounds (data not shown). However, the binding modes for two more bulky aromatic compounds (indoxyl sulfate in the PDB entry 2BXH and thyroxine in the PDB entry 1HK4) are located either within site CypA (2BXH) or right between sites CypA and CypB (1HK4).

The above results show that independent molecular modeling confirmed the possibility of two different nonoverlapping binding sites for cypate in complex with albumin, one being more hydrophobic than the other. These sites, denoted here as CypA (hydrophilic) and CypB (hydrophobic), do not coincide with the sites characteristic for binding of small compounds and, perhaps, with sites suggested by specific labeling of albumin in Sudlow *et al.* (41). However, our molecular modeling did not fully account for all details of cypate–albumin interaction including possible conformational changes in albumin upon binding cypate.

CONCLUSION

Molecular modeling reveals that albumin has two binding sites responsible for binding of polymethine dyes, denoted here as CypA and CypB. The binding sites differ in their polarities and affect the fluorescence lifetime of the bound probes. The alteration in binding sites changes the pocket polarity and therefore impacts the lifetimes as well as fluorescent fractional contributions. Thus, both the lifetime and fractional contributions represent a set of conformationally sensitive parameters which could be utilized in high-throughput screening of albumin and potentially whole blood to identify abnormalities associated with certain pathologies.

REFERENCES

1. Caraceni, P., A. Gasbarrini, D. H. Van Thiel and A. B. Borle (1994) Oxygen free radical formation by rat hepatocytes during postanoxic reoxygenation: Scavenging effect of albumin. *Am. J. Physiol.* **266**, G451–G458.
2. Iglesias, J. and J. S. Levine (2001) Albuminuria and renal injury—beware of proteins bearing gifts. *Nephrol. Dial. Transplant.* **16**, 215–218.
3. Watanabe, A., S. Matsuzaki, H. Moriwaki, K. Suzuki and S. Nishiguchi (2004) Problems in serum albumin measurement and clinical significance of albumin microheterogeneity in cirrhotics. *Nutrition* **20**, 351–357.
4. Ivanov, A. I., E. A. Korolenko, E. V. Korolik, S. P. Firsov, R. G. Zhbankov, M. K. Marchewka and H. Ratajczak (2002) Chronic liver and renal diseases differently affect structure of human serum albumin. *Arch. Biochem. Biophys.* **408**, 69–77.
5. Gryzunov, T. A., T. I. Syrejshchikova, M. N. Komarova, E. Y. Misionzhnik, M. G. Uzbekov, A. V. Molodetskich, G. E. Dobretsov and M. N. Yakimenko (2000) Serum albumin binding sites properties in donors and in schizophrenia patients: The study of fluorescence decay of the probe K-35 using S-60 synchrotron pulse excitation. *Nucl. Instrum. Methods Phys. Res. A* **448**, 478–482.
6. Kazmierczak, S. C., A. Gurachevsky, G. Matthes and V. Muravsky (2006) Electron spin resonance spectroscopy of serum albumin: A novel new test for cancer diagnosis and monitoring. *Clin. Chem.* **52**, 2129–2134.
7. Dobson, C. M. (2004) Experimental investigation of protein folding and misfolding. *Methods* **34**, 4–14.
8. Huang, B. X., C. Dass and H. Y. Kim (2005) Probing conformational changes of human serum albumin due to unsaturated fatty acid binding by chemical cross-linking and mass spectrometry. *Biochem. J.* **387**, 695–702.
9. Chattopadhyay, K. and C. Frieden (2006) Steady-state and time-resolved fluorescence studies of the intestinal fatty acid binding protein. *Proteins* **63**, 327–335.
10. Marme, N., J. P. Knemeyer, M. Sauer and J. Wolfrum (2003) Inter- and intramolecular fluorescence quenching of organic dyes by tryptophan. *Bioconjug. Chem.* **14**, 1133–1139.

11. Bloch, S., F. Lesage, L. McIntosh, A. Gandjbakhche, K. Liang and S. Achilefu (2005) Whole-body fluorescence lifetime imaging of a tumor-targeted near-infrared molecular probe in mice. *J. Biomed. Opt.* **10**, 054003.

12. Lee, H., J. C. Mason and S. Achilefu (2006) Heptamethine cyanine dyes with a robust C-C bond at the central position of the chromophore. *J. Org. Chem.* **71**, 7862–7865.

13. Lichtman, J. W. and J. A. Conchello (2005) Fluorescence microscopy. *Nat. Methods* **2**, 910–919.

14. Kuwana, E. and E. M. Sevick-Muraca (2002) Fluorescence lifetime spectroscopy in multiply scattering media with dyes exhibiting multiexponential decay kinetics. *Biophys. J.* **83**, 1165–1176.

15. Ntziachristos, V. and R. Weissleder (2002) Charge-coupled-device based scanner for tomography of fluorescent near-infrared probes in turbid media. *Med. Phys.* **29**, 803–809.

16. Achilefu, S., R. B. Dorshow, J. E. Bugaj and R. Rajagopalan (2000) Novel receptor-targeted fluorescent contrast agents for in vivo tumor imaging. *Invest. Radiol.* **35**, 479–485.

17. Mason, J. C. (2001) *The Synthesis of Novel Near-Infrared Heptamethine Cyanine Dyes*. Ph.D. thesis. Georgia State University, Atlanta, GA.

18. Peters, T. J. (1996) *All About Albumin: Biochemistry, Genetics, and Medical Applications*. Academic Press, New York.

19. Vakser, I. A. (1996) Low-resolution docking: Prediction of complexes for underdetermined structures. *Biopolymers* **39**, 455–464.

20. Ye, Y., S. Bloch, J. Kao and S. Achilefu (2005) Multivalent carbocyanine molecular probes: Synthesis and applications. *Bioconjug. Chem.* **16**, 51–61.

21. Selinger, B. K. and C. M. Harris (1983) The pile-up problem in pulse fluorometry. *NATO ASI Ser., A, Life Sci.* **69**, 115–127.

22. Tayyab, S., N. Sharma and M. M. Khan (2000) Use of domain specific ligands to study urea-induced unfolding of bovine serum albumin. *Biochem. Biophys. Res. Commun.* **277**, 83–88.

23. Kang, Y. N., H. Kim, W. S. Shin, G. Woo and T. W. Moon (2003) Effect of disulfide bond reduction on bovine serum albumin-stabilized emulsion gel formed by microbial transglutaminase. *J. Food Sci.* **68**, 2215–2220.

24. Cohn, E. J., L. E. Strong, W. L. Hughes Jr, D. J. Mulford, J. N. Ashworth, M. Melin and H. L. Taylor (1946) Preparation and properties of serum and plasma proteins. IV. A system for the separation into fractions of the protein and lipoprotein components of biological tissues and fluids. *J. Am. Chem. Soc.* **68**, 459–475.

25. Matejtschuk, P., C. H. Dash and E. W. Gascoigne (2000) Production of human albumin solution: A continually developing colloid. *Br. J. Anaesth.* **85**, 887–895.

26. Schneider, W., H. Lefevre, H. Fiedler and L. J. McCarty (1975) Alternative method of large scale plasma fractionation for the isolation of serum albumin. *Blut* **30**, 121–134.

27. Togashi, D. M. and A. G. Ryder (2006) Time-resolved fluorescence studies on bovine serum albumin denaturation process. *J. Fluoresc.* **16**, 153–160.

28. Chatelain, P., J. R. Matteazzi and R. Laruel (1994) Binding of fantofarone, a novel Ca^{2+} antagonist, to serum albumin—a fluorescence study. *J. Pharm. Sci.* **83**, 674–676.

29. Barik, A., K. I. Priyadarsini and H. Mohan (2003) Photophysical studies on binding of curcumin to bovine serum albumin. *Photochem. Photobiol.* **77**, 597–603.

30. Abugo, O. O., P. Herman and J. R. Lakowicz (2001) Fluorescence properties of albumin blue 633 and 670 in plasma and whole blood. *J. Biomed. Opt.* **6**, 359–365.

31. Abugo, O. O., R. Nair and J. R. Lakowicz (2000) Fluorescence properties of rhodamine 800 in whole blood and plasma. *Anal. Biochem.* **279**, 142–150.

32. Jisha, V. S., K. T. Arun, M. Hariharan and D. Ramaiah (2006) Site-selective binding and dual mode recognition of serum albumin by a squaraine dye. *J. Am. Chem. Soc.* **128**, 6024–6025.

33. Geddes, C. D., H. Cao, I. Gryczynski, Z. Gryczynski, J. Y. Fang and J. R. Lakowicz (2003) Metal-enhanced fluorescence (MEF) due to silver colloids on a planar surface: Potential applications of indocyanine green to in vivo imaging. *J. Phys. Chem. A* **107**, 3443–3449.

34. Sudlow, G., D. J. Birkett and D. N. Wade (1976) Further characterization of specific drug binding sites on human serum albumin. *Mol. Pharmacol.* **12**, 1052–1061.

35. Curry, S., H. Mandelkow, P. Brick and N. Franks (1998) Crystal structure of human serum albumin complexed with fatty acid reveals an asymmetric distribution of binding sites. *Nat. Struct. Biol.* **5**, 827–835.

36. Bhattacharya, A. A., T. Grune and S. Curry (2000) Crystallographic analysis reveals common modes of binding of medium and long-chain fatty acids to human serum albumin. *J. Mol. Biol.* **303**, 721–732.

37. Ghuman, J., P. A. Zunszain, I. Petitpas, A. A. Bhattacharya, M. Otagiri and S. Curry (2005) Structural basis of the drug-binding specificity of human serum albumin. *J. Mol. Biol.* **353**, 38–52.

38. Lejon, S., I. M. Frick, L. Bjorck, M. Wikstrom and S. Svensson (2004) Crystal structure and biological implications of a bacterial albumin binding module in complex with human serum albumin. *J. Biol. Chem.* **279**, 42924–42928.

39. Yang, F., C. Bian, L. Zhu, G. Zhao, Z. Huang and M. Huang (2007) Effect of human serum albumin on drug metabolism: Structural evidence of esterase activity of human serum albumin. *J. Struct. Biol.* **157**, 348–355.

40. Bloch, S., B. Xu, Y. Ye, K. Liang, G. V. Nikiforovich and S. Achilefu (2006) Targeting Beta-3 integrin using a linear hexapeptide labeled with a near-infrared fluorescent molecular probe. *Mol. Pharm.* **3**, 539–549.

41. Sudlow, G., D. J. Birkett and D. N. Wade (1975) The characterization of two specific drug binding sites on human serum albumin. *Mol. Pharmacol.* **11**, 824–832.